Ultranarrow bandwidth nonlinear Faraday optical filter at rubidium D_2 transition

Wei Zhuang (庄 伟)*, Yelong Hong (洪叶龙), Zhiwen Gao (高智文), Chuanwen Zhu (祝传文), and Jingbiao Chen (陈景标)

State Key Laboratory of Advanced Optical Communication System and Network, School of Electronics Engineering and Computer Science, Peking University, Beijing 100871, China

**Corresponding author: wzhuang@pku.edu.cn*

Received May 21, 2014; accepted July 25, 2014; posted online September 26, 2014

We demonstrate a narrowband optical filter which operates on the $5^2S_{1/2}$ to $5^2P_{3/2}$ transition at 780 nm in rubidium vapor based on optical-pumping-induced dichroism combined with Faraday anomalous dispersion effects. Its peak transmission is 18.4(2)% at the $5^2S_{1/2}$, $F = 2$ to $5^2P_{3/2}$, $F' = 1, 3$ crossover transition, whereas at the $5^2S_{1/2}$, $F = 2$ to $5^2P_{3/2}$, $F' = 2, 3$ crossover transition the transmission is 18.6(2)%. Both transitions have a bandwidth (full-width at half-maximum of peak transmission) as narrow as 24.5(8) MHz, which is remarkably improved compared with the narrowest bandwidth as we know. This technique can also be applied to other alkali atoms.

OCIS codes: 120.2440, 230.2240, 300.6460.
doi: 10.3788/COL201412.101204.

Faraday anomalous dispersion optical filter (FADOF) has many advantages: high transmission, ultranarrow bandwidth[1], and high noise rejection[2]. Hence, FADOF is used in many fields where signal-to-noise ratio (SNR) is critical, such as free-space optical communication[3], lidar[4–7], and the generation of narrowband quantum light[8]. And optical filter can be used for optical frequency stabilization when adopted as a frequency selection component in laser system[9–13]. So far, FADOF has been widely studied both theoretically and experimentally with several elements, including rubidium (Rb)[14–21], potassium[22,23], cesium[24,25], sodium[26,27], and calcium[28].

However, the bandwidth of FADOF is generally limited at gigahertz level due to Doppler broadening. Thus, an excited state atomic filter based on circular dichroism is realized[29,30]. Pumping laser is used to induce circular dichroism rather than magnetic field. In recent years, based on various novel methods, the bandwidth of the optical filter reduces to 80[31], 61[32], and 60 MHz[20] in Rb vapor.

For laser frequency stabilization, narrower bandwidth and higher transmission provide a better locking signal and therefore the laser can be stabilized to a higher precision. In this letter, with the help of Faraday anomalous dispersion effects, we present a nonlinear optical filter with narrower bandwidth than that previously reported. The mechanisms we used are the Faraday effect, saturated absorption, and circular dichroism[31,32]. Polarization directions of those transitions selected by saturation effects rotate and pass through the orthogonal polarizers, not being absorbed totally. Eventually, we realize a filter with bandwidth of 24.5(8) MHz.

Figure 1 shows the ^{87}Rb D_2 transition hyperfine structure. The 780 nm laser can be tuned to cover all of the $5^2S_{1/2}$ to $5^2P_{3/2}$ transitions of Rb. The natural linewidth of $5^2P_{3/2}$ state is 6 MHz[33].

The experimental setup is shown in Fig. 2. We use an optical isolator (ISO) to suppress the optical feedback. Laser beam from external cavity diode laser (ECDL) is divided into two parts by a beam splitter (BS) evenly: one part is used for saturated absorption spectra (SAS) as a standard reference where the Rb cell is pure Rb (with 27.2% ^{87}Rb and 72.8% ^{85}Rb) and the other part passes through a half-wave plate (HWP) to change the polarization direction. Polarization BS (PBS) divides laser into two, a strong one as pump beam and a weak one as probe beam. Neutral density filter (NDF) is used to change the intensity of pump laser. Quarter-wave plate (QWP) turns linear polarization into circular polarization. M_1, M_2, M_3, and M_4 are high reflection mirrors for 780 nm. G_1 and G_2 are polarization-orthogonal Glan–Taylor prisms with an extinction ratio 10^5:1. The pure ^{87}Rb cell is 5 cm long. It is controlled by a heating circuit and the temperature can be adjusted

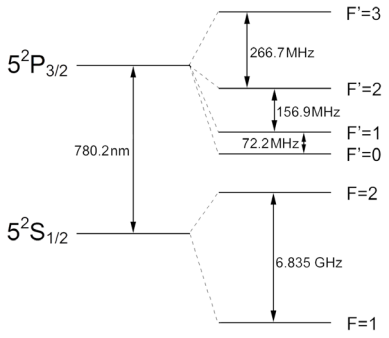

Fig. 1. ^{87}Rb D_2 transition hyperfine structure.

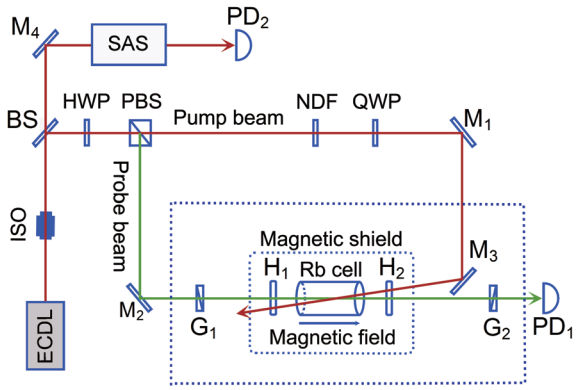

Fig. 2. Experimental setup.

up to 150 °C. A magnetic field along the axis of the Rb vapor is applied by two permanent magnets (H). The magnetic field can be adjusted by changing the distance between the two permanent magnets. Photodiode (PD) collects light when it travels through the nonlinear optical filter.

The transmitted spectra of Rb $5^2S_{1/2}$ to $5^2P_{3/2}$ transition are illustrated in Fig. 3. The saturated absorbed spectra (upper curve) are reference signals which contain ^{87}Rb and ^{85}Rb. The transmitted spectra without pump are indicated by red dashed lines. The probe laser frequency can be swept over 10 GHz which can demonstrate the transmitted spectra of Rb D_2 transition of both ^{87}Rb and ^{85}Rb. Figures 3(a) and (b) (partial enlarged) show transmitted spectra when the magnetic field is adjusted to 11 G and the temperature of vapor cell is controlled to 58 °C with the pump laser intensity of 0.68 mW/cm^2 corresponding to the Rabi frequency of $2\pi \times 2.74$ MHz. The center frequencies of the nonlinear optical filter pass bands coincide with Rb $5^2S_{1/2}$ to $5^2P_{3/2}$ SAS shown as the upper curve in Fig. 3. The transmission of $5^2S_{1/2}$, $F = 2$ to $5^2P_{3/2}$, $F' = 1, 3$ crossover transition is 5.2(1)%, and the $5^2S_{1/2}$, $F = 2$ to $5^2P_{3/2}$, $F' = 2, 3$ crossover transition is 6.7(1)%. It should be noted that the transmitted spectra demonstrates pass bands corresponding to the ^{87}Rb SAS. However, residual ^{85}Rb atoms in the pure ^{87}Rb would also induce pass bands when heated to a high temperature, which is disadvantageous for laser frequency stabilization on the ^{87}Rb transition line.

In Figs. 3(c) and (d) (partial enlarged), the temperature of the vapor cell is increased to 85 °C while other parameters keep the same values. From Figs. 3(c) and (d), we observe that the transmission of $5^2S_{1/2}$, $F = 2$ to $5^2P_{3/2}$, $F' = 1, 3$ crossover transition achieves 18.4(2)%, and the transmission of $5^2S_{1/2}$, $F = 2$ to $5^2P_{3/2}$, $F' = 2, 3$ crossover transition gets to 18.6(2)%. Meanwhile, we deduce the full-width at half-maximum (FWHM) bandwidth of both $5^2S_{1/2}$, $F = 2$ to $5^2P_{3/2}$, $F' = 1, 3$ crossover transition and $5^2S_{1/2}$, $F = 2$ to $5^2P_{3/2}$, $F' = 2, 3$ crossover transition pass bands to be 24.5 MHz by the

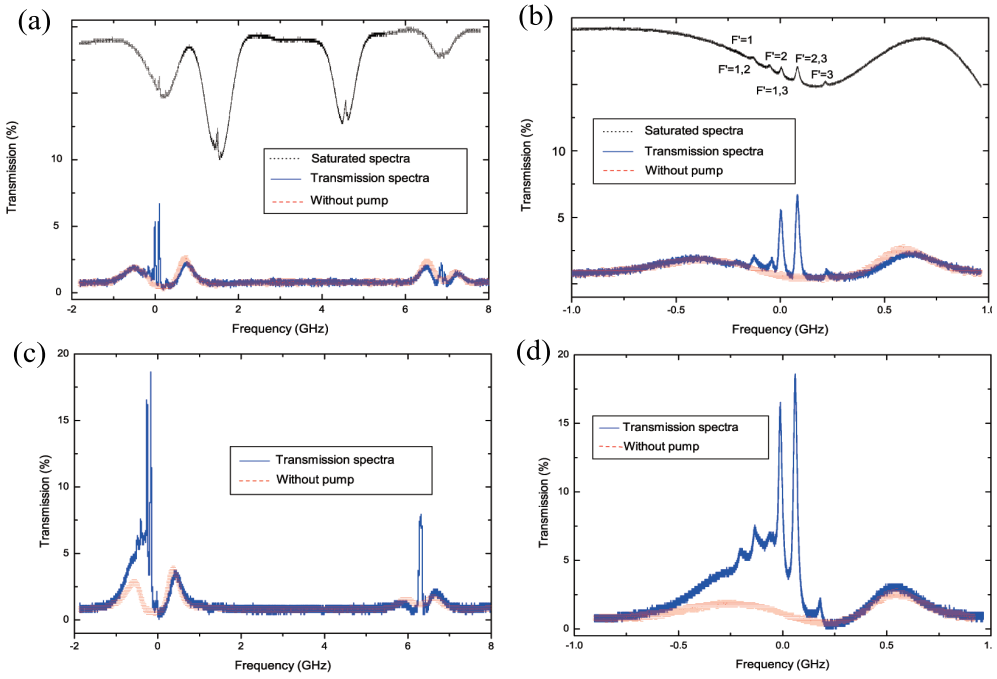

Fig. 3. Transmitted spectra of $5^2S_{1/2}$ to $5^2P_{3/2}$ transition (solid blue line). Transmitted spectra without pump (dashed red line). The upper dotted curves are reference saturated absorbed spectra collected by PD_2: (a) $5^2S_{1/2}$, $F = 2$ to $5^2P_{3/2}$, $F' = 1, 2, 3$ and $5^2S_{1/2}$, $F = 1$ to $5^2P_{3/2}$, $F' = 0, 1, 2$ transitions at 11 G and 58 °C with pump intensity 0.68 mW/cm^2; (b) $5^2S_{1/2}$, $F = 2$ to $5^2P_{3/2}$, $F' = 1, 2, 3$ transitions at 11 G and 58 °C with pump intensity 0.68 mW/cm^2; (c) $5^2S_{1/2}$, $F = 2$ to $5^2P_{3/2}$, $F' = 1, 2, 3$ and $5^2S_{1/2}$, $F = 1$ to $5^2P_{3/2}$, $F' = 0, 1, 2$ transitions at 11 G and 85 °C with pump intensity 0.68 mW/cm^2; (d) $5^2S_{1/2}$, $F = 2$ to $5^2P_{3/2}$, $F' = 1, 2, 3$ transitions at 11 G and 85 °C with pump intensity 0.68 mW/cm^2.

frequency reference signal of SAS. The background signal without pump shown in Fig. 3 is caused by the Faraday anomalous dispersion effects of the bias magnetic field and will disappear if two permanent magnets are removed. Nevertheless, it will not affect the frequency stability when applied to laser frequency stabilization.

We also investigate the dependence of the nonlinear optical filter transmission on the parameters of temperature, pump intensity, and magnetic field for the Rb vapor cell in Fig. 4. The solid lines represent the transmission of $5^2S_{1/2}$, $F = 2$ to $5^2P_{3/2}$, $F' = 1, 3$ pass band and dashed lines represent that of $5^2S_{1/2}$, $F = 2$ to $5^2P_{3/2}$, $F' = 2, 3$ pass band. As shown in Fig. 4(a), when the pump intensity is 0.68 mW/cm^2 and the magnetic field is 11 G, the transmission increases with the temperature of the Rb vapor cell. However, the transitions reach the maximum at 85 °C, and begin to decrease when the temperature is increased further. It means that the increasing absorption of the pump beam in the cell starts to reduce the dichroism for the probe beam when the temperature exceeds 85 °C. Figure 4(b) shows the variations of the transmissions while changing the pump intensity and the temperature is kept at 85 °C and magnetic field at 11 G. It is obvious that the transmissions increase with the pump laser intensity and get to saturation gradually. Limited to our laser output power, the pump intensity is maintained at 0.68 mW/cm^2. Figure 4(d) shows the dependence of the FWHM bandwidth on the pump intensity. The bandwidth of the Faraday optical filter broadens when increasing the pump intensity. Therefore, there is a trade-off between the transmission and the bandwidth of the Faraday optical filter.

Figure 4(c) shows that the bias magnetic field applied in the experiment affects the transmissions significantly. The temperature is still set to 85 °C and pump intensity is at 0.68 mW/cm^2. When changing the magnetic field intensity, the transmissions begin to increase at first, maintain large values subsequently, and decrease rapidly at last. The maximum transmissions of $5^2S_{1/2}$, $F = 2$ to $5^2P_{3/2}$, $F' = 1, 3$ transition and $5^2S_{1/2}$, F = 2 to $5^2P_{3/2}$, $F' = 2, 3$ transition are 19.7% and 15.1%, respectively, when the magnetic field is set to 5 G. Actually, the transmission of the nonlinear Faraday optical filter is proportional to $\Delta v_B/[(\Delta v_B)^2 + (\Gamma/2)^2]$, where Δv_B is the Zeeman splitting and Γ is the frequency linewidth of pumped atoms. Therefore, the transmission keeps increasing with the bias magnetic field when Δv_B is smaller than $\Gamma/2$. It reaches the maximum when Δv_B equals $\Gamma/2$. The transmission drops out when Δv_B further exceeds $\Gamma/2$ shown in Fig. 4(c). Besides, the irregular fluctuations of the transmissions may be caused by the inhomogeneity of the bias magnetic field which could be improved if the permanent magnets are replaced by coils. To sum up, the transmissions of the nonlinear optical filter can be improved with the help of a bias magnetic field and will be beneficial for laser frequency stabilization.

In conclusion, we demonstrate an ultranarrow bandwidth optical filter at 780 nm Rb transition. The filter

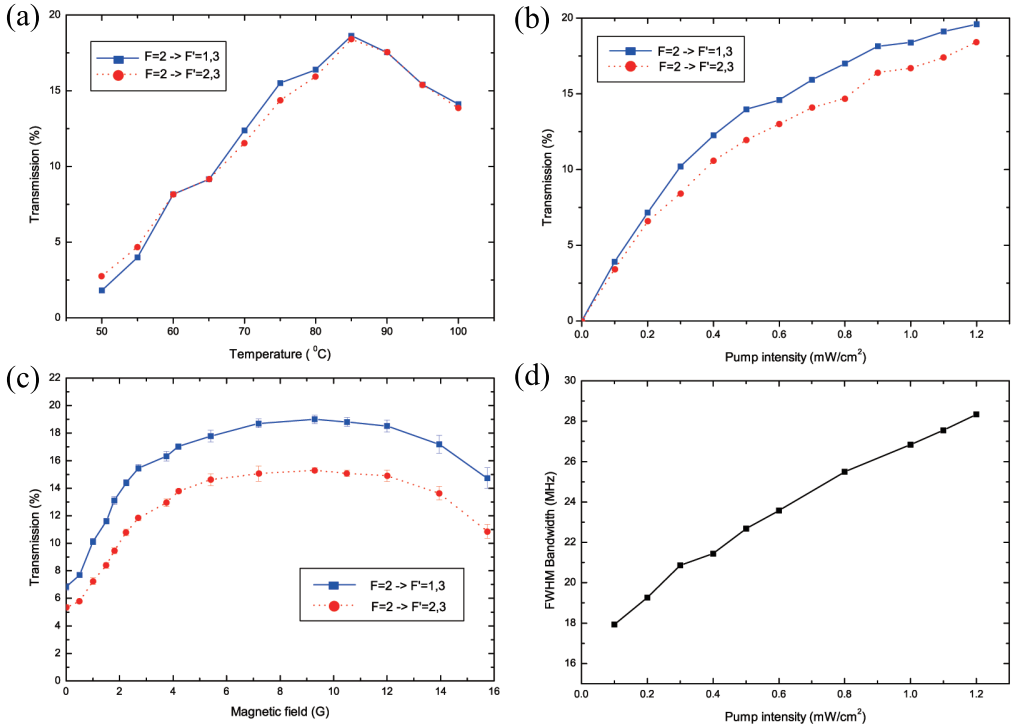

Fig. 4. Dependence of transmission of $5^2S_{1/2}$, $F = 2$ to $5^2P_{3/2}$, $F' = 1, 3$ transition (solid line) and $5^2S_{1/2}$, $F = 2$ to $5^2P_{3/2}$, $F' = 2, 3$ (dashed line) on (a) temperature; (b) pump intensity; (c) magnetic field. (d) Dependence of bandwidth on pump intensity.

achieves a peak transmission of 18.4(2)% at $5^2S_{1/2}$, $F = 2$ to $5^2P_{3/2}$, $F' = 1$, 3 crossover transition and of 18.6(2)% at $5^2S_{1/2}$, $F = 2$ to $5^2P_{3/2}$, $F' = 2$, 3 crossover transition at 11 G and 58 °C with pump intensity 0.68 mW/cm^2. Both the transitions have the same narrow bandwidth of 24.5(8) MHz. It should be noted that, once the pumping laser is locked to a fixed frequency, there is only one single transmission peak and the transition bandwidth is exactly the FWHM of peak transition. We realize an external cavity laser using a conventional FADOF with gigahertz bandwidth, which is immune to current and temperature fluctuations. Based on this work, we can realize an external cavity laser operating within the frequency range of 20 MHz, also immune to current and temperature fluctuations. Additionally, the filter can be applied to laser frequency stabilization.

This work was supported by the National Natural Science Foundation of China (Nos. 10874009 and 11074011) and the National 863 Program of China.

References

1. J. Menders, K. Benson, S. H. Bloom, C. S. Liu, and E. Korevaar, Opt. Lett. **11,** 846 (1991).
2. D. J. Dick and T. M. Shay, Opt. Lett. **16,** 867 (1991).
3. J. Tang, Q. Wang, Y. Li, L. Zhang, J. Gan, M. Duan, J. Kong, and L. Zheng, Appl. Opt. **34,** 2619 (1995).
4. J. Höffner and C. Fricke-Begemann, Opt. Lett. **30,** 890 (2005).
5. A. Popescu and T. Walther, Appl. Phys. **98,** 667 (2010).
6. A. Popescu, K. Schorstein, and T. Walther, Appl. Phys. B **79,** 955 (2004).
7. A. Popescu, D. Walldorf, K. Schorstein, and T. Walther, Opt. Commun. **264,** 475 (2006).
8. J. S. Neergaard-Nielsen, B. M. Nielsen, H. Takahashi, A. I. Vistnes, and E. S. Polzik, Opt. Express **15,** 7940 (2007).
9. K. Choi, J. Menders, P. Searcy, and E. Korevaar, Opt. Commun. **96,** 240 (1992).
10. X. Miao, L. Yin, W. Zhuang, B. Luo, A. Dang, J. Chen, and H. Guo, Rev. Sci. Instrum. **82,** 086106 (2011).
11. X. Zhang, Z. Tao, C. Zhu, Y. Hong, W. Zhuang, and J. Chen, Opt. Express **21,** 28010 (2013).
12. L. Wang, Z. Tian, Y. Zhang, J. Wang, S. Fu, J. Sun, and Q. Wang, Chin. Opt. Lett. **10,** 011402 (2012).
13. K. Ko, K. Lee, H. Park, J. Han, Y. Cha, G. Lim, T. Kim, and D. Jeong, Chin. Opt. Lett. **10,** S21903 (2012).
14. Z. Hu, X. Sun, X. Zeng, Y. Peng, J. Tang, L. Zhang, Q. Wang, and L. Zheng, Opt. Commun. **101,** 175 (1993).
15. M. Duan, Y. Li, J. Tang, and L. Zheng, Opt. Commun. **127,** 210 (1996).
16. Q. Sun, W. Zhuang, Z. Liu, and J. Chen, Opt. Lett. **36,** 4611 (2011).
17. X. Xue, Z. Tao, Q. Sun, Y. Hong, W. Zhuang, B, Luo, J. Chen, and H. Guo, Opt. Lett. **37,** 2274 (2012).
18. J. A. Zielińska, F. A. Beduini, N. Godbout, and M. W. Mitchell, Opt. Lett. **37,** 524 (2012).
19. Q. Sun, Y. Hong, W. Zhuang, Z. Liu, and J. Chen, Appl. Phys. Lett. **101,** 211102 (2012).
20. X. Shan, X. Sun, J. Luo, and M. Zhan, Opt. Lett. **33,** 1842 (2008).
21. H. Guo, A. Dang, Y. Han, S. Gao, Y. Cao, and B. Luo, Chin. Sci. Bull. **55,** 527 (2010).
22. E. T. Dressler, A. E. Laux, and R. I. Billmers, J. Opt. Soc. Am. B **13,** 1849 (1996).
23. Y. Zhang, X. Jia, Z. Ma, and Q. Wang, Opt. Commun. **194,** 147 (2001).
24. Y. Wang, S. Zhang, D. Wang, Z. Tao, Y. Hong, and J. Chen, Opt. Lett. **37,** 4059 (2012).
25. Y. Wang, X. Zhang, D. Wang, Z. Tao, W. Zhuang, and J. Chen, Opt. Express **20,** 25817 (2012).
26. H. Chen, C. Y. She, P. Searcy, and E. Korevaar, Opt. Lett. **18,** 1019 (1993).
27. H. Chen, M. A. White, David A. Krueger, and C. Y. She, Opt. Lett. **21,** 1093 (1996).
28. Y. C. Chan and J. Gelbwachs, IEEE J. Quant. Electron. **29,** 2379 (1993).
29. S. K. Gayen, R. I. Billmers, V. M. Contarino, M. F. Squicciarini, W. J. Scharpf, G. Yang, P. R. Herczfeld, and D. M. Allocca, Opt. Lett. **20,** 1427 (1995).
30. S. Liu, Y. Zhang, H. Wu, and D. Fan, Opt. Commun. **284,** 4180 (2011).
31. A. Cerè, V. Parigi, M. Abad, F. Wolfgramm, A. Predojević, and M. W. Mitchell, Opt. Lett. **34,** 1012 (2009).
32. S. Liu, Y. Zhang, H. Wu, and P. Yuan, Opt. Commun. **285,** 1181 (2012).
33. D. A. Steck, "Rubidium 87 d line data," http://steck.us/alkalidata (2009).